16th World Conference on Earthquake, 16WCEE 2017
Santiago Chile, January 9th to 13th 2017
Paper N° 1898
Registration Code: S-K1464631708

DUCTILITY AND SHEAR DEMANDS IN REINFORCED CONCRETE BUILDINGS WITH ASYMMETRIC WALLS

A. Morales G.(1)(2), P. Ceresa(3), M. A. Hube(4)

(1) *PhD Candidate, UME School, Istituto Universitario di Studi Superiori di Pavia (IUSS), 27100, Italy, jose.morales@umeschool.it*
(2) *Associate Professor, School of Civil Engineering, Universidad de Valparaíso, Valparaíso, Chile*
(3) *Assistant Professor, Istituto Universitario di Studi Superiori di Pavia (IUSS), Pavia, 27100, Italy, paola.ceresa@iusspavia.it*
(4) *Associate Professor, Department of Structural and Geotechnical Engineering and National Research Center for Integrated Natural Disaster Management CONICYT/FONDAP/15110017, Pontificia Universidad Católica de Chile, mhube@ing.puc.cl*

Abstract

This research aims to obtain envelopes of the ductility and shear demands in reinforced concrete (RC) wall buildings subjected to ground motions. These envelopes could be used in the future to provide design recommendations for RC wall buildings. A case study building with asymmetric walls (i.e. with non-rectangular cross sections) designed according to Eurocode 8 is analysed. In order to evaluate the seismic performance of the building, nonlinear response history analysis (NRHA) with increasing levels of ground motion intensity was performed. The asymmetric RC walls are modelled with two different approaches. The first model is characterised by concentrated inelasticity (MCI), since it considers the nonlinear behaviour only at the base of the walls. The second is a model with distributed inelasticity (MDI), which considers that the nonlinear behaviour can take place at any building level if the demand is larger than the wall yield capacity. In both modelling cases the nonlinear behaviour of the wall is represented using the tri-linear SINA hysteretic rule, calibrated with available experimental data. The computed distribution of the bending moments and shear forces along the wall height presents a significant discrepancy between MCI and MDI. However, the results obtained with the MDI are consistent with the provided moment strength. Finally, the curvature ductility demands at the base of the wall predicted by both models are similar. The main discrepancy between the two models is that ductility demands above the base of the walls are predicted by the MDI when the intensity of excitation increases.

Keywords: Reinforced concrete; Asymmetric walls; Ductility demands; Shear demands; Seismic behaviour

1. Introduction

Reinforced concrete (RC) structural walls are one of the most commonly employed lateral-load resisting systems for mid- and high-rise buildings. Structural engineers often use structural walls in buildings, since their large stiffness and strength enable them to carry large lateral loads due to wind and earthquakes while also minimizing lateral displacements.

Due to architectural and structural reasons, the use of non-rectangular or asymmetric walls (C-, T-, and L-shapes) in buildings is common where there is the need of a constant subdivision of floor areas in all storeys. In these types of buildings, T- and C-shaped walls are used to define the corridors, residential units or elevator cores [1, 2].

Most of the available analytical studies of ductility and shear demands in RC walls buildings use a single cantilever wall as a simplification to represent the whole building, and assume that the nonlinear behaviour is concentrated at the critical section (base) of the wall, while the rest of the wall is assumed to behave elastically [3, 4]. Given the assumption of an elastic response above the critical section, the bending moments in such regions are not bounded, while the bending moment at the base is bounded by the provided moment strength. Since the practice of structural engineering is based on design codes that specify design envelopes for bending moments (e.g. Eurocode 8 [5], NZS 3101 [6], CSA A23.3 [7]), obtaining elastic response and unbounded bending moments above the base of the walls is an unrealistic situation under severe earthquakes.

The main aim of this work is to obtain envelopes of the ductility and shear demands in RC building with asymmetric walls. This paper presents a numerical study of a research building that represents a real structure. The seismic response under severe earthquakes is estimated, considering the particularities of the cyclic behaviour of asymmetric walls.

The asymmetric RC walls are modelled with two different approaches. The first model is characterised by concentrated inelasticity (MCI), since it considers the nonlinear behaviour only at the base of the walls. The second is a model with distributed inelasticity (MDI), which considers that the nonlinear behaviour can take place at any building level if the demand is larger than the wall yield capacity. Therefore, the stiffness is a function of the strength of the wall at each level, and that the yield curvature is constant along the wall height [8]. The hysteretic force-deformation relationship used to represent the cyclic behaviour of the asymmetric walls was calibrated with available experimental data [9, 10, 11, 12], as it will be discussed in the following sections.

2. Case study building

The floor plan view of the case study building is shown in Fig. 1, T-shaped and C-shaped RC walls are used to resist lateral loads in both directions. The building has ten storeys with a constant inter-storey height of 3.0 m; the thickness of the walls is 0.3 m.

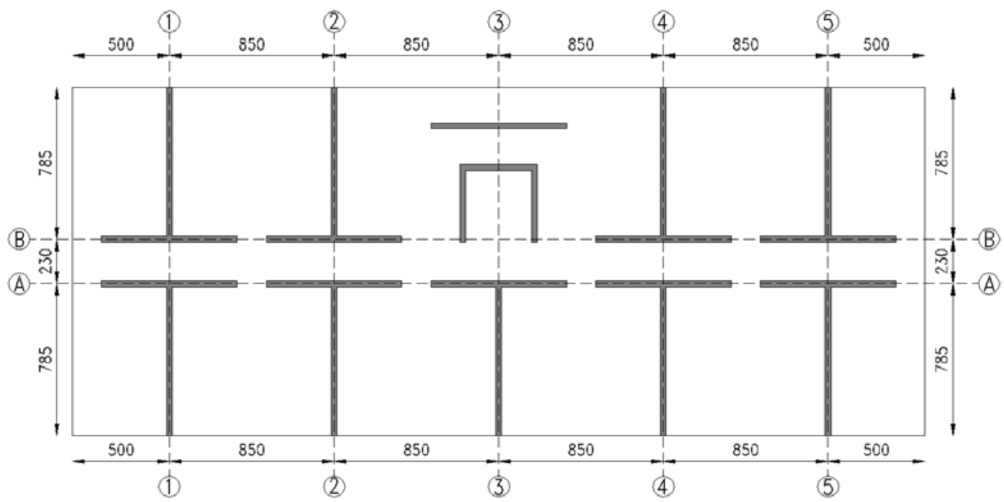

Fig. 1 – Plan view of the ten-storey case study building (dimensions in centimeters)

The building was designed according to Eurocode 8 (EC8) [5]. A type “C” soil (dense sand or gravel, or stiff clay) was used in conjunction with 0.4g design ground acceleration, considering a high seismicity area. The concrete and reinforcement material properties adopted for the seismic design are typical values of the engineering practice. The selected values for reinforcing yield strength (f_y) and characteristic compressive strength of concrete (f'_c) are 500 MPa and 30 MPa, respectively.

Table 1 summarises the main design outputs of the T-shaped walls and the C-shaped wall, where ρ_L is the longitudinal reinforcement ratio, q is the behaviour factor for uncoupled wall systems of high ductility class, and N is the factored axial load in the wall. The design base shear of the buildings was 14000 kN, 17% of the seismic weight.

Table 1 – Longitudinal reinforcing ratios and axial load ratios

	T-shaped wall		**C-shaped wall**	
q	ρ_L [%]	$N/A_g f'_c$	ρ_L [%]	$N/A_g f'_c$
4.4	0.5	0.04	0.5	0.05

3. Analytical models of the buildings

The seismic performance of the research building was assessed using two-dimensional (2D) nonlinear response history analysis (NRHA) using the finite-element software RUAUMOKO 2D [13], which mainly uses lumped plasticity beam elements to study the behavior of RC elements. For all the structural members, the flexural nonlinear behavior is considered, while the shear behavior is assumed to be linearly elastic, with stiffness based on the effective shear area of the members.

Fig. 2 shows a two-component beam element, where the two members in parallel represent the behaviour of the element. One member is elastic and the second one is also elastic but with a perfect hinge at one end or both ends of the member [13]. The nonlinear behaviour is achieved assigning a hysteretic model to the perfect hinge. In this work, the walls are modelled with two-component beam element with hinges at both ends.

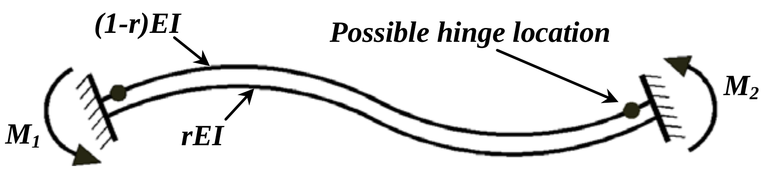

Fig. 2 – Two-component beam element, adapted from [13]

The nonlinear behavior of RC walls is represented using the tri-linear SINA hysteretic model [14] to represent the moment-rotation relationship at each of the two hinges. This rule is shown in Fig. 3a and consists on a tri-linear backbone with stiffness changes at cracking and yielding (F_y^+, F_y^-). According to the SINA hysteresis rule, the cracked stiffness and the cracked moments or forces (F_{cr}^+, F_{cr}^-), can be distinct in the two loading directions, allowing thus the modeling of asymmetric sections. In addition, pinching effect is considered trough the definition of the crack closing moment or force (F_{cc}).

Using available experimental data of asymmetric RC walls subjected to cyclic loads reported by Thomsen and Wallace [12] (named TW-1, TW-2), Sittipunt and Wood [11] (CLS, CMS), Beyer *et al*. [9] (TUA, TUB), and Brueggen [10] (NTW1, NTW2), the RC wall model was calibrated achieving a good representation of the cyclic behavior of the tested asymmetric RC wall specimens. A correlation between the parameters that define the hysteresis rule and the experimental results was determined. For each specimen the tri-linear backbone was obtained directly from the moment-curvature relationship while the crack closing moment (F_{cc}) was defined through a trial and error procedure. The results are shown in Fig. 3b. The comparison between the experimental behavior and the predicted response for two specimens is shown in Fig. 4, where the proposed model is able to predict the cyclic response adequately.

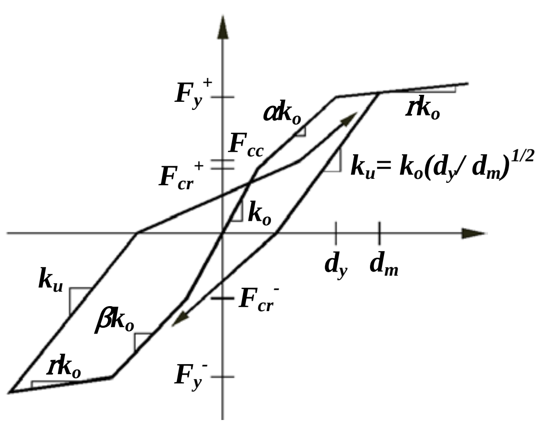

a)

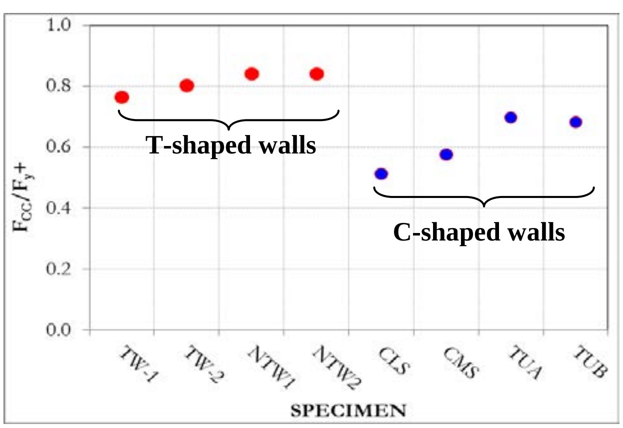

b)

Fig. 3 – a) Tri-linear SINA hysteretic rule, adapted from [13], and b) correlation between SINA parameters and experimental results

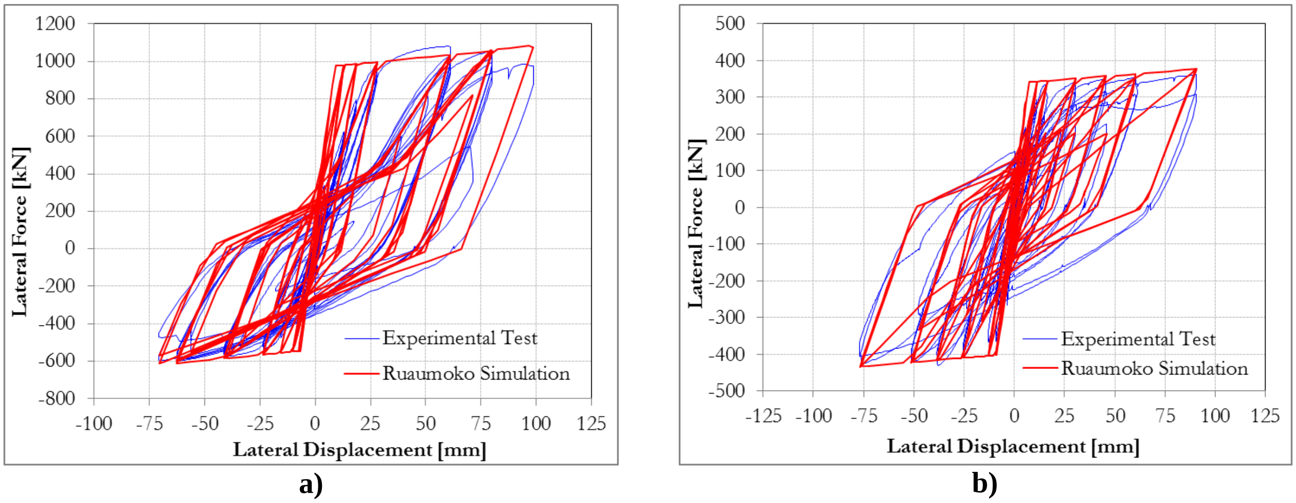

Fig. 4 – Comparison between the analytical model and experimental results: a) T-shaped wall (NTW2) after Brueggen [10], and b) C-shaped wall (TUB) after Beyer *et al.* [9]

3.1 Building model

The two-dimensional model of the building is shown in Fig. 5, where all axes are modelled simultaneously. The walls were modelled with two-node elements with the hysteretic behaviour previously described. The effective slabs connecting the two walls in each axis, were modelled using two-node beam elements, located at member centroids. End offsets are considered in the effective slabs to account for the wall widths. The Takeda hysteresis rule was used for modeling the effective slab sections whereas the tri-linear SINA hysteretic rule was adopted for walls.

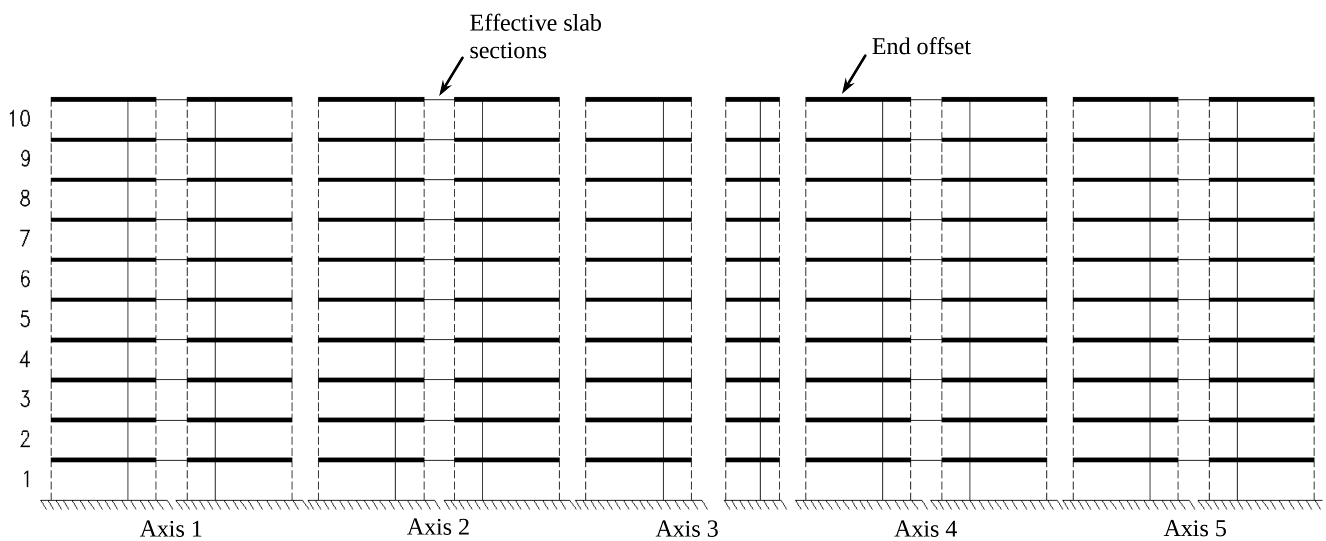

Fig. 5 – RUAUMOKO 2D structural model of the building

Two different modeling assumptions for the walls were considered in this study. First, a model with concentrated inelasticity (MCI), that considers the nonlinear behavior only at the base of the wall [3 4], while elastic response is considered above the critical section (see Fig. 6a). For this modeling case, the bending moments are not bounded at the upper storeys. The second approach used in this work is a model with distributed inelasticity (MDI), which considers that the nonlinear behavior can take place anywhere in the wall if the demand is larger than the yield capacity. The MDI model of one wall is shown in Fig. 6b, where four two-component beam elements are considered at each storey, in order to obtain a better representation of the lateral displacement profile and lateral stiffness. Since the inelastic behaviour is lumped in discrete points along the wall height (perfect hinge of two-component beam element), a static pushover analysis of the T-shaped wall was carried out in RUAMOKO 2D and its results were compared with those obtained with a fibre beam model, implemented in SeismoStruct [15]. It is observed that the lateral stiffness and yield deformation of the wall are predicted with reasonable accuracy, for the flange in compression (FiC) and the flange in tension (FiT), as shown in Fig. 7. Therefore, the discretization proposed for MDI is able to predict the behavior of the wall adequately.

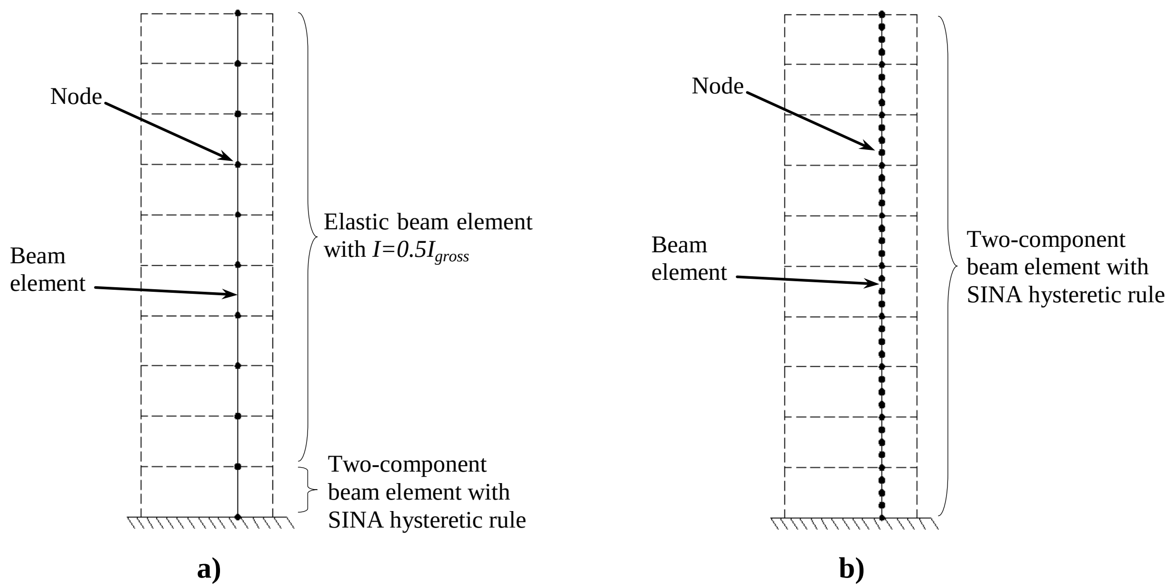

Fig. 6 – Two wall models: (a) MCI and (b) MDI

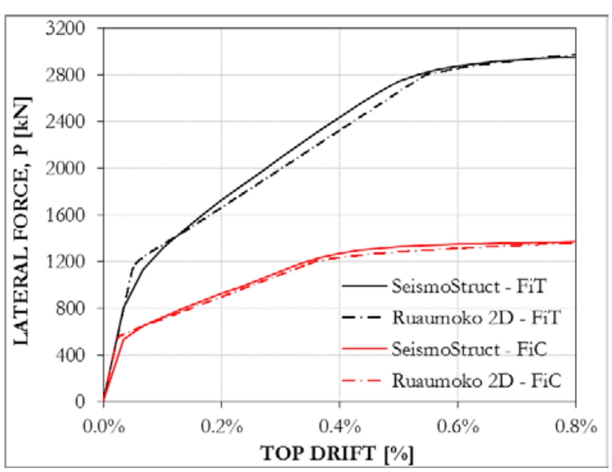

Fig. 7 – Pushover analysis of the T-shaped wall (where FiT stays for Flange in Tension, FiC for Flange in Compression)

4. Considered Ground Motions

In this work, nine ground motions selected by Maley *et al*. [16] were used to estimate the seismic demand of the building. Table 2 lists the details of the considered ground motions where the scale factors correspond to an average intensity of a_g=0.4 g. The pseudo-acceleration and displacement response spectra of the considered set of ground motions are shown in Fig. 8. It is observed that the median response spectrum of the set of ground motions provides a good match to the target spectrum of Eurocode 8 [5] used to design the research building.

Table 2 – Ground motions and scaling factors used by Maley *et al*. [16]

Earthquake Name	**Earthquake Magnitude**	**PGA (g)**	**V_{s30} (m/s)**	**Scaling Factor**	**Component**
Chi-Chi	7.62	0.09	273	3.4	CHICHI/TAP042-E
Landers	7.28	0.15	345	3.9	LANDERS/DSP090
Hector	7.13	0.06	345	5.2	HECTOR/0534c270
Darfield	7.10	0.06	-	7.3	N00E
Loma Prieta	6.93	0.09	271	3.6	LOMAP/SJW160
Kobe	6.90	0.06	256	3.5	KOBE/OSA090
Superstition Hills-02'	6.54	0.18	208	1.8	SUPERST/B-IVW090
Imperial Valley-06	6.53	0.35	275	1.6	IMPVALL/H-DLT352
Chi-Chi Taiwan-03	6.20	0.05	226	7.0	CHICHI03/CHY055-W

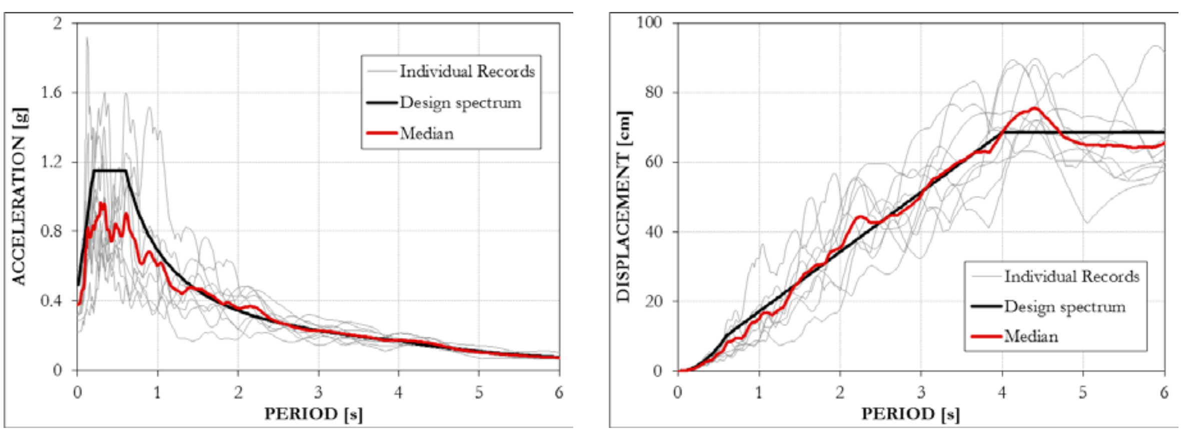

a) b)

Fig. 8 – 5% damped spectra for the nine ground motions considered: a) pseudo-acceleration, and b) displacement

5. Results

The seismic demands of the T-shaped walls are presented hereafter since the global response of the building depends mainly on the response of these walls (see Fig. 1). The seismic performance of the research building was assessed from two-dimensional (2D) nonlinear response history analysis (NRHA). Fig. 9a shows the drift demands of the T-shaped wall of axis 1 (Fig. 1) of the building obtained using the MCI (with nonlinear behaviour at the base of the wall only) for the ten selected ground motions. The average drift demand is also shown. Fig. 9b presents the drift demands estimated with the MDI (with nonlinear behaviour along the wall height). In the upper storeys, it is observed that the maximum drift demands are similar for the two models, while, at the lower levels, the drift demands are smaller in the MDI.

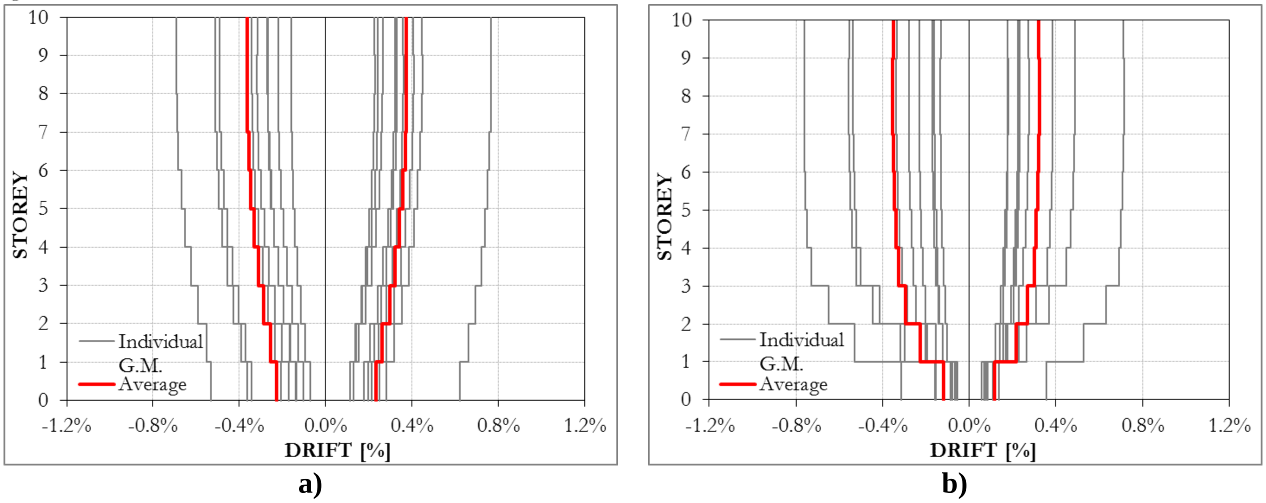

Fig. 9 – Drift demand in T-shaped wall: a) MCI and b) MDI (where G.M. stays for ground motion)

The bending moment diagram for the T-shaped wall of axis 1 for the MCI and MDI are shown in Fig. 10a and 10b, respectively. Because the stiffness of the wall in upper storeys is constant in the MCI, the values of the bending moments are similar in both directions, i.e. for flange in tension (FiT) or for flange in compression (FiC). However, at lower storeys the bending moments in both directions are different because they are limited to the provided strength at the base of the wall, which is different in both directions due to the asymmetric cross-section of the wall. The flexural strength in the direction of the flange in tension is larger than for the flange in compression. Therefore, moment demands larger than the base moment are observed above the critical section in Fig. 10a for the walls with the flange in compression.

Fig. 10b shows the bending moment demands for the MDI. As the stiffness of the wall is associated with the provided moment strength, the distribution of the bending moments along the wall height is different than that of the MCI, and the bending moments are bounded by the yield moments at each level of the wall. The yield bending moments in both directions are shown with a black line in Fig. 10b. It is observed that the bending moment demands are lower when the flange is in compression and its values decrease along the wall height.

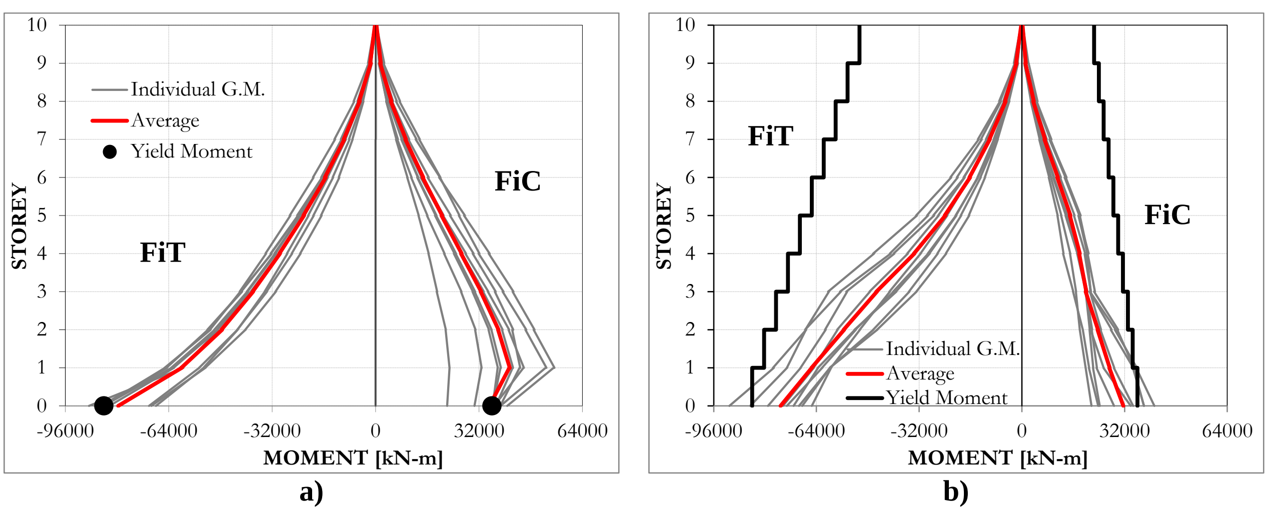

Fig. 10 – T-shaped wall moments over height: a) MCI and b) MDI

Fig. 11a shows the shear demands in the T-shaped walls of axis 1 obtained with the MCI. It is observed that the maximum shear takes place at the first level. However, at levels above the base, the shear demands decrease. At the upper storeys the shear demands are similar in both directions of the walls. For MDI the predicted maximum shear demands are smaller than those of the MCI and take place at the first four levels. Furthermore, a different distribution of the shear forces along the wall height is observed in Fig. 11b, where larger shear demand is predicted if the flange of the wall is in tension; this result is consistent with the lateral stiffness of the wall.

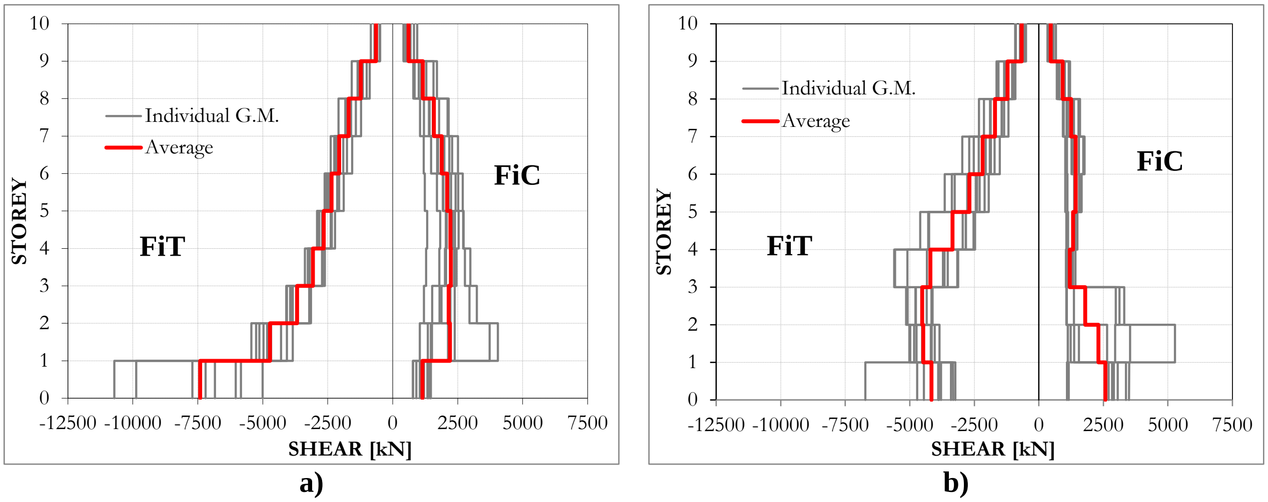

Fig. 11 – T-shaped wall shears over height: a) MCI and b) MDI

Fig. 9 shows that the displacement profile of the research building is consistent with a response dominated by the first inelastic mode [8] with plastic hinge at the base of the walls in most cases. Furthermore, the bending moment diagram (Fig. 10) does not have amplification at mid-height of the wall, which is the typical influence of the higher-mode effects. Investigations into the response of single cantilever walls [4] have showed that, when the intensity of excitation increases, the influence of higher-mode effects in amplifying the envelopes of wall moments and shear also increased [8].

In order to evaluate the influence of the excitation intensity in the response of the research building, NRHAs were performed using the selected records (Table 2) scaled to 150% and 200% of the design intensity. The bending moment demands of the T-shaped walls are shown in Fig. 12a and 12b for an intensity ratio IR = 1.5, and in Fig. 12c and 12d for an intensity ratio IR = 2.0. When the MCI is considered, the moment demands at the base of the wall are larger than the yield moment, as shown in Fig. 10a. However, the average values of the moment demands along the wall height are similar to the results obtained for the design intensity (IR = 1.0). In the case of the MDI for IR = 2.0, nonlinear behavior above the critical section is observed until the second level for the wall with FiC. However the moments decrease along the wall height; in the case of MDI, the average values of the moment demands increase with respect to the results obtained for the design intensity (IR = 1.0), as shown Fig. 10b.

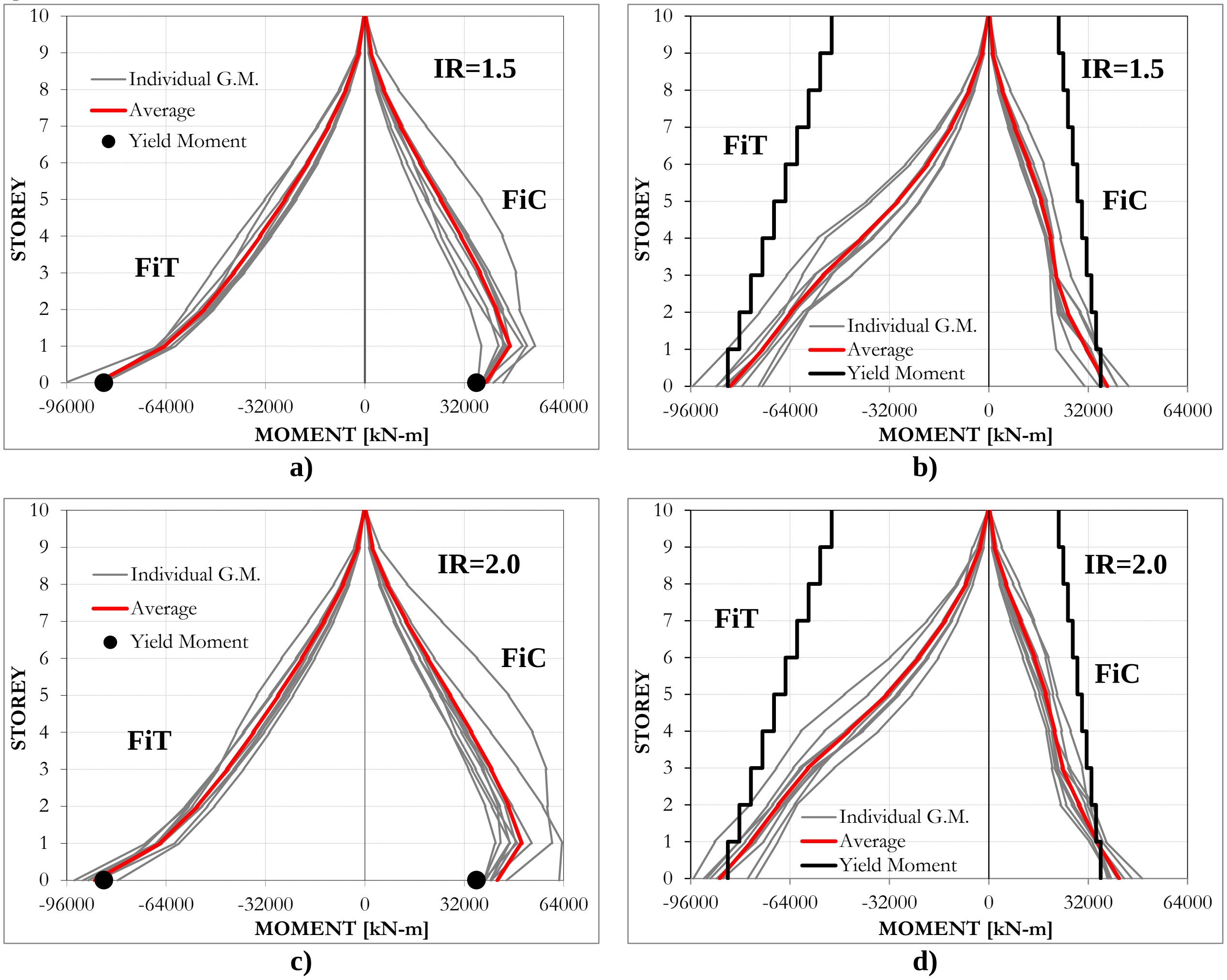

Fig. 12 – T-shaped wall moments over height: a), c) MCI, and b), d) MDI

Despite the intensity of excitation is increased, the shape and values of the bending moment diagrams do not change so much with respect to the design intensity (IR = 1.0); the distribution of the moments along the wall height is consistent with a response controlled mainly by the first inelastic mode. Therefore, without higher-mode effects, the shear demands depend essentially on the provided moment strength at the base of the wall. The shear demands along the wall height for intensity ratios 1.5 and 2.0 are shown in Fig. 13. Considering the MCI, the average values of the shear demands obtained for the three different intensity levels are basically the same, as shown Fig. 11a, 13a, and 13c. The same effect can be observed for the MDI, where the average of the shear demands remains practically constant for the three studied intensity levels, as shown Fig. 11b, 13b, and 13d.

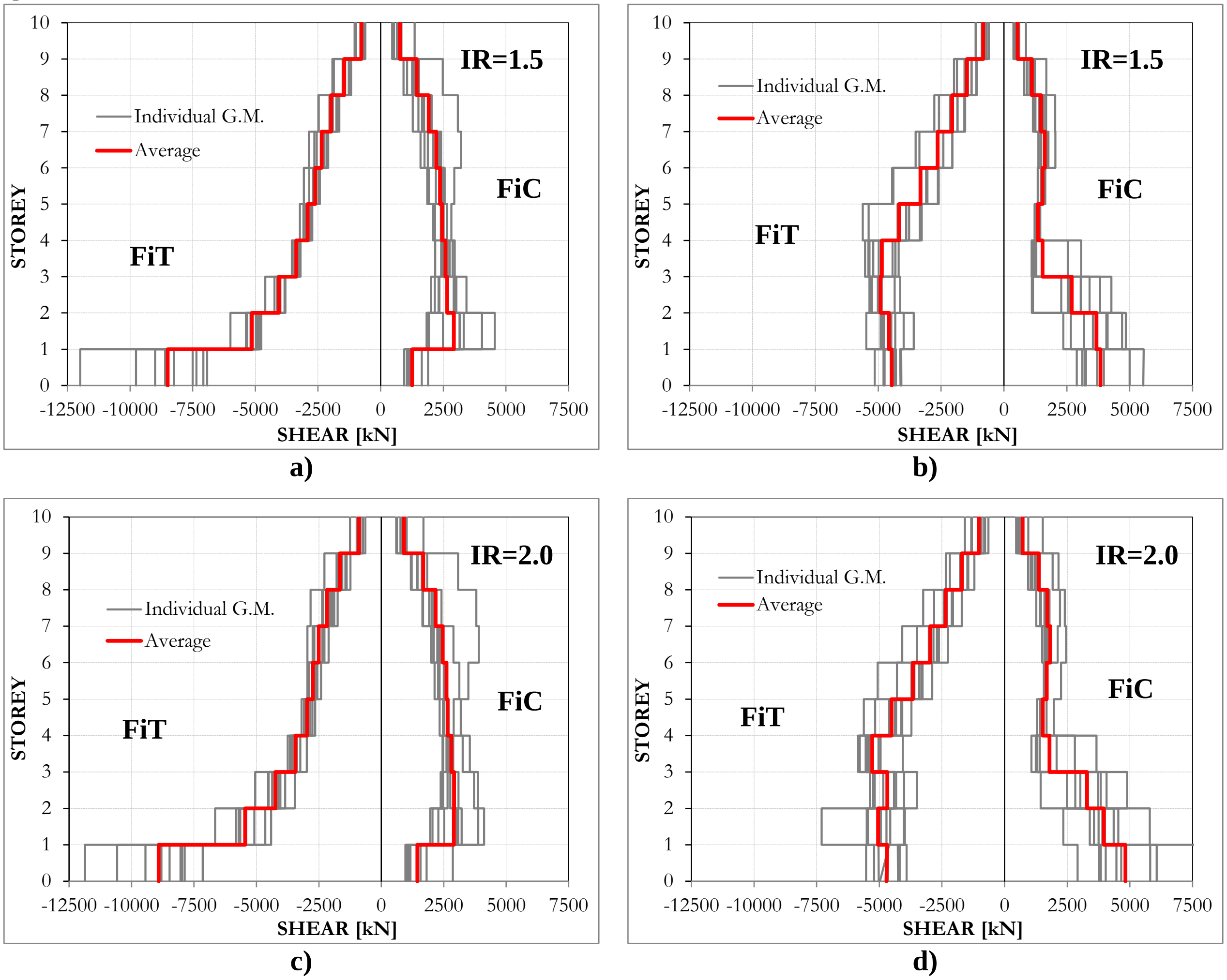

Fig. 13 – T-shaped wall shears over height: a), c) MCI, and b), d) MDI

Finally, the curvature ductility demands of the T-shaped walls for the three different intensity levels, and for the two modeling cases, are presented in Fig. 14. It is observed that similar ductility demands are predicted by both models at the base of the walls. However, the main discrepancy between the two models is that the ductility demands above the base of the walls are predicted by the MDI when the excitation intensity increases. In fact ductility demands of 5 and 2 are observed in the first and second level, respectively.

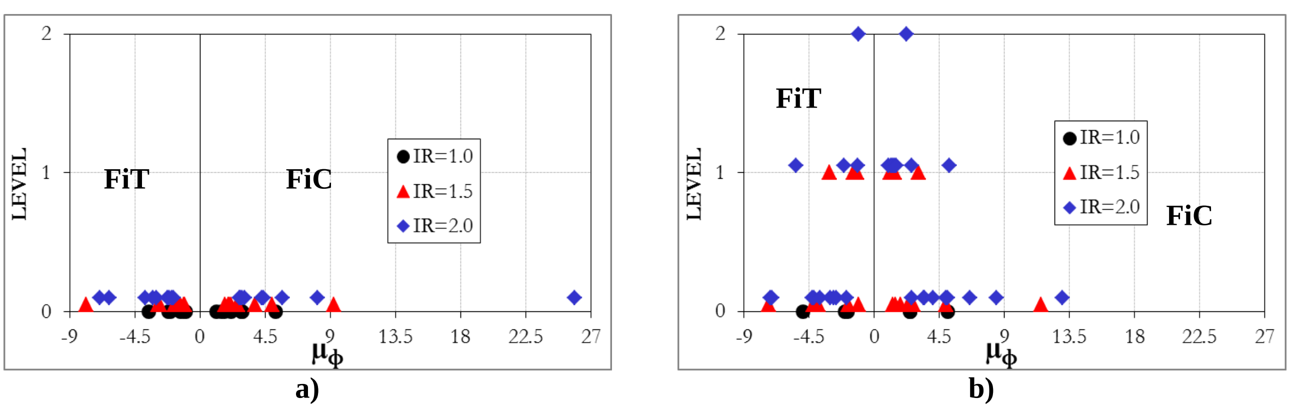

Fig. 14 – T-shaped wall curvature ductility demands: a) MCI and b) MDI

6 Conclusions

Due to the asymmetry in its properties, the behaviour of studied walls differs considerably from that of rectangular walls. Asymmetric walls exhibit particular characteristics in terms of strength and stiffness, depending of the direction of loading, which need to be accounted for in the design.

In this work, a 10-storey RC building with asymmetric walls was designed according to Eurocode 8 [5] and its seismic performance was assessed from nonlinear response history analysis, performed for three different ground motion intensity levels, and two models for representing the behaviour of the walls, a model with concentrated inelasticity (MCI) and a model with distributed inelasticity (MDI), respectively.

The main two differences between MCI and MDI are the inelasticity at the upper storeys and the lateral stiffness along the wall height. The stiffness of the MCI is constant, whereas it becomes a function of the strength of the wall for the MDI. Therefore, the distribution of the bending moments and shear forces is different between the two considered models.

According the shear and moment demands obtained in this work, it is inferred that the models used to evaluate the seismic behaviour of RC building with asymmetric walls should account for the different stiffness of the wall in each direction, and the provided strength of the wall along the wall height. Based on the obtained results, the MDI adopted in this work is a reasonable and simple alternative to the models with concentrated inelasticity.

For the MCI, two problems are detected. First, this model cannot predict potential nonlinear behaviour above the critical section of the wall, overestimating the moment demands at the upper storeys. The second problem is the lateral stiffness. The MCI considered the same stiffness in each direction of the wall at the upper storeys. This is an unrealistic assumption for asymmetric walls, therefore, the distribution of the shear and moment demands are not consistent with the real stiffness of the wall.

To analyze RC walls, it is important to model appropriately the cracked stiffness of the wall, since this stiffness determines base shear, storey drifts, and internal force distributions (moment and shear demands). Many design codes specify the cracked wall stiffness as a fraction of the gross-section stiffness. This approach does not consider that for asymmetric walls the cracked stiffness is different in each direction. The designer should pay attention to the provided moment strength in the direction of analysis, in order to estimate the cracked stiffness of asymmetric walls adequately.

7. Acknowledgements

The first author acknowledges the support of the Becas Chile Programme (CONICYT) in form of PhD scholarship.

8. References

[1] Moehle J (2015): *Seismic design of reinforced concrete buildings*. McGraw-Hill Education.

[2] Alarcón C, Hube M, Junemann R, de la Llera J (2015): Characteristics and displacement capacity of reinforced concrete walls in damaged buildings during 2010 Chile earthquake. *Bulletin of Earthquake Engineering*, **13** (4), 1119-1139.

[3] Pennucci D, Sullivan TJ, Calvi GM (2015): Inelastic higher-mode response in reinforced concrete wall structures. *Earthquake Spectra*, **31** (3), 1493–1514.

[4] Priestley N, Amaris A (2002): Dynamic amplification of seismic moments and shear forces in cantilever walls. *Research Report ROSE – 2002/01*, IUSS press, Pavia, Italy.

[5] CEN (2004): Eurocode 8 – Design of structures for earthquake resistance- Part 1: General rules, seismic actions and rules for buildings, *EN 1998-1*, European Committee for Standardization, Brussels, Belgium.

[6] NZS (2006): NZS 3101 - Concrete Structures Standard Part 1 (Standard) and Part 2(Commentary), Standards New Zealand.

[7] CSA (2004): CSA Standard A23.3-04 - Design of concrete structures, Canadian Standards Association, Toronto, Ont.

[8] Priestley MJN, Calvi GM, Kowalsky MJ (2007): *Displacement-Based Seismic Design of Structures*. IUSS Press, Pavia, Italy.

[9] Beyer K, Dazio A, Priestley MJN (2008): Quasi-static cyclic tests of two U-shaped reinforced concrete walls. *Journal of Earthquake Engineering*, **12** (7), 1023-1053.

[10] Brueggen B L (2009): Performance of T-shaped Reinforced Concrete Structural Walls under Multi-Directional Loading. *Ph.D Thesis*, University of Minnesota.

[11] Sittipunt C, Wood S (1993): Finite Element Analysis of Reinforced Concrete Shear Walls. *A Report to the National Science Foundation*, Research Grant BCS 89-12992.

[12] Thomsen JH, Wallace JW (1995): Displacement-Based Design of RC Structural Walls: Experimental Studies of Walls with Rectangular and T-shaped Cross Sections. *Report No.CU/CEE-95/96*, Department of Civil and Environmental Engineering, Clarkson University, 353 pp.

[13] Carr AJ (2012): Ruaumoko Manual – Volume 3: User manual for the 3-dimensional version Ruaumoko3D. Department of Civil Engineering, University of Canterbury, Christchurch, New Zealand.

[14] Saiidi M, Sozen M (1979): Simple and complex model for nonlinear seismic response of reinforced concrete structures. *A Report to the National Science Foundation*, Research Grant PFR 78-16318.

[15] Seismosoft (2013): SeismoStruct v6.5 – A computer program for static and dynamic nonlinear analysis of framed structures. Available from http://www.seismosoft.com

[16] Maley TJ, Sullivan TJ, Lago A, Roldan R, Calvi GM (2013): Characterising the Seismic Behaviour of Steel MRF Structures. *Report 2013/02*, IUSS Press, Pavia, Italy.